

- 6) Chi JH, McDermott MW : Tuberculum sellae meningiomas. *Neurosurg Focus* **14** : Article 6, 2003
- 7) Cook SW, Smith Z, Kelly DF : Endonasal transsphenoidal removal of tuberculum sellae meningiomas : technical note. *Neurosurgery* **55** : 239-246, 2004
- 8) Divitiis Ed, Cavallo LM, Esposito F, Stella L, Messina A : Extended endoscopic transsphenoidal approach for tuberculum sellae meningiomas. *Neurosurgery* **61** (ONS Suppl 2) : ONS529-ONS538, 2007
- 9) Divitiis Ed, Esposito F, Cappabianca P, Cavallo LM, Divitiis Od : Tuberculum sellae meningiomas : high route or low route? A series of 51 consecutive cases. *Neurosurgery* **62** : 556-563, 2008
- 10) Fahlbusch R, Schott W : Pterional surgery of meningiomas of the tuberculum sellae and planum sphenoidale : surgical results with special consideration of ophthalmological and endocrinological outcomes. *J Neurosurg* **96** : 235-243, 2002
- 11) Fatemi N, Dusick JR, Neto MAdP, Malkasian D, Kelly DF : Endonasal versus supraorbital keyhole removal of craniopharyngiomas and tuberculum meningiomas. *Neurosurgery* **64** (supple 2) : 269-284, 2009
- 12) Frank G, Pasquini E : Tuberculum sellae meningioma : the extended transsphenoidal approach-for the virtuoso only? *World Neurosurg* **73** : 625-626, 2010
- 13) Galal A, Faisal A, Al-Werdany M, Shehaby AE, Lotfy T, Moharram H : Determinants of postoperative visual recovery in suprasellar meningiomas. *Acta Neurochir (Wien)* **152** : 69-77, 2010, August 26 Epub, 2009
- 14) Ganna A, Dehdashti AR, Karabatsou K, Gentili F : Fonto-basal interhemispheric approach for tuberculum sellae meningiomas ; long-term outcome. *Br J Neurosurg* **23** : 422-430, 2009
- 15) Gardner PA, Kassam AB, Thomas A : Endoscopic endonasal resection of anterior cranial base meningiomas. *Neurosurgery* **63** : 36-52, 2008
- 16) Goel A, Muzumdar D, Desai KI : Tuberculum sellae meningioma : A report on management on the basis of a surgical experience with 70 patients. *Neurosurgery* **51** : 1358-1364, 2002
- 17) 長谷川光広 : 視神経, 視交叉近傍髄膜腫の手術手技—視機能改善のために—. *脳外速報* **19** : 1372-1378, 2009
- 18) Ito Z : The microsurgical interhemispheric approach suitably applied to ruptured aneurysms of the anterior communicating artery in the acute stage. *Acta Neurochir (Wien)* **63** : 85-99, 1982
- 19) Jallo GI, Benjamin V : Tuberculum sellae meningiomas : microsurgical anatomy and surgical technique. *Neurosurgery* **51** : 1432-1440, 2002
- 20) Kadis GN, Mount AL, Ganti SR : The importance of early diagnosis and treatment of the meningiomas of the planum sphenoidale and tuberculum sellae : A retrospective study of 105 cases. *Surg Neurol* **12** : 367-371, 1979
- 21) Kassam A, Carrau RL, Snyderman CH, Gardner P, Mintz A : Evolution of reconstructive techniques following endoscopic expanded endonasal approaches. *Neurosurg Focus* **19** : E8, 2005
- 22) Kassam AB, Thomas A, Carrau RL, Snyderman CH, Vescan A, Prevedelle D, Mintz A, Gardner P : Endoscopic reconstruction of the cranial base using a pedicled nasoseptal flap. *Neurosurgery* **63** (ONS Supple 1) : ONS44-ONS53, 2008
- 23) Kato T, Sawamura Y, Abe H, Nagashima M : Transsphenoidal-transtuberculum sellae approach for supradiaphragmatic tumors : technical note. *Acta Neurochir (Wien)* **140** : 715-718, 1998
- 24) Kitano M, Taneda M, Nakao Y : Postoperative improvement in visual function in patients with tuberculum sellae meningiomas : results of the extended transsphenoidal and transcranial approaches. *J Neurosurg* **107** : 337-346, 2007
- 25) Kobayashi H, Asaoka K, Terasaka S, Murata J-i : Primary closure of a cerebrospinal fluid fistula by nonpenetrating titanium clips in endoscopic endonasal transsphenoidal surgery : Technical note. *Skull Base* **21** : 47-52, 2011
- 26) Kunicki A, Uhl A : The clinical picture and results of surgical treatment of meningioma of the tuberculum sellae. *Cesk Neurol* **31** : 80-91, 1968
- 27) Li X, Liu M, Liu Y, Zhu S : Surgical management of tuberculum sellae meningiomas. *J Clin Neurosci* **14** : 1150-1154, 2007
- 28) mahmoud M, Nader R, Al-Mefty O : Optic canal involvement in tuberculum sellae meningiomas : influence on approach, recurrence, and visual recovery. *Neurosurgery* **66** (ONS Supple 1) : ONS108-ONS119, 2010
- 29) Margalit NS, Lesser JB, Moche J, Sen C : Meningiomas involving the optic nerve : technical aspects and outcomes for a series of 50 patients. *Neurosurgery* **53** : 523-532, 2003
- 30) Mathiesen T, Kihlstrom L : Visual outcome of tuberculum sellae meningiomas after extradural optic nerve decompression. *Neurosurgery* **59** : 570-576, 2006
- 31) 師井淳太, 波出石弘, 石川達哉, 澤田元史, 鈴木明文, 安井信之 : Basal interhemispheric approach における大脳半球間裂剝離のトレーニングレジデントが陥る軟膜損傷のパターンとその対策. *脳卒中の外科* **36** : 367-372, 2008
- 32) Nakamura M, Roser F, Struck M, Vorkapic P, Samii M : Tuberculum sellae meningiomas : clinical outcome considering different surgical approaches. *Neurosurgery* **59** : 1019-1029, 2006
- 33) Nozaki K, Kikuta K-i, Takagi Y, Mineharu Y, Takahashi JA, Hashimoto N : Effect of early optic canal unroofing on the outcome of visual functions in surgery for meningiomas of the tuberculum sellae and planum sphenoidale. *Neurosurgery* **62** : 839-846, 2008
- 34) Otani N, Muroi C, Yano H, Khan N, Pangalu A, Yonekawa Y : Surgical management of tuberculum sellae meningiomas : Role of selective extradural anterior clinoidectomy. *Br J Neurosurg* **20** : 129-138, 2006
- 35) Pamir MN, Ozduman K, Belirgen M, Kilic T, Ozek MM : Outcome determinates of pterional surgery for tuberculum sellae meningiomas. *Acta Neurochir (Wien)* **147** : 1121-1130, 2005

2005

- 36) Park C-K, Jung H-W, Yang S-Y, Seol HJ, Paek SH, Kim DG : Surgically treated tuberculum sellae and diaphragm sellae meningiomas : The importance of short-term visual outcome. *Neurosurgery* **59** : 238-243, 2006
- 37) Schick U, Hassler W : Surgical management of tuberculum sellae meningiomas : involvement of the optic canal and visual outcome. *J Neurol Neurosurg Psychiatry* **76** : 977-983, 2005
- 38) Solero CL, Giombini S, Morello G : Suprasellar and olfactory meningiomas. Report on a series of 153 personal cases. *Acta Neurochir (Wien)* **67** : 181-194, 1983
- 39) 鈴木明文, 安井信之 : 前交通動脈瘤に対する interhemispheric approach. *脳外誌* **1** : 218-225, 1992
- 40) 谷川緑野, 小林 徹, 林 恵充, 泉 直人, 橋爪 明, 藤田 力, 橋本政明 : 前交通動脈動脈瘤に対する interhemispheric approach の利点と手術手技上のポイント. *脳卒中の外科* **30** : 208-212, 2002
- 41) 寺坂俊介, 岩崎喜信, 黒田 敏, 内田隆徳 : ポリグルコール酸不織布フェルトとフィブリン糊による新しい硬膜閉鎖法—臨床応用 140 例の結果—. *No Shinkei Geka* **34** : 1109-1117, 2006
- 42) Terasaka S, Iwasaki Y, Shinya N, Uchida T : Fibrin glue and polyglycolic acid non-woven fabric as a biocompatible dural substitute. *Neurosurgery* **58** : ONS134-ONS139, 2006
- 43) Terasaka S, Asaoka K, Kobayashi H, Yamaguchi S : Anterior interhemispheric approach for tuberculum sellae meningioma. *Neurosurgery* **68** (ONS Supple 1) : ONS 84-ONS 89, 2010
- 44) Zevgaridis D, Medele RJ, Muller A, Hischa AC, Steiger HJ : Meningiomas of the sellar region presenting with visual impairment : impact of various prognostic factors on surgical outcome in 62 patients. *Acta Neurochir (Wien)* **143** : 471-476, 2001

胆管細胞癌よりの脈絡叢転移性腫瘍の1例*

栗栖 宏多¹⁾, 鴨嶋 雄大¹⁾, 寺坂 俊介¹⁾, 小林 浩之¹⁾, 久保田 佳奈子²⁾, 寶金 清博¹⁾

A Case of Metastatic Choroid Plexus Tumor from Cholangiocellular Carcinoma

Kota KURISU¹⁾, Yuuta KAMOSHIMA¹⁾, Shunsuke TERASAKA¹⁾, Hiroyuki KOBAYASHI¹⁾,
Kanao KUBOTA²⁾, and Kiyohiro HOUKIN¹⁾

Key words :

metastatic tumor,
intraventricular tumor,
choroid plexus,
Ber EP-4,
cholangiocellular carcinoma

Metastatic intraventricular tumor located in the choroid plexus is very rare. Only a few cases have been reported in the past. According to past reports, these tumors originated from lung, colon, and so on, but not from the bile duct. This is the first case report of choroid plexus metastasis from cholangiocellular carcinoma.

A 57-year-old woman who had a history of cholangiocellular carcinoma, demonstrated intraventricular tumor. Although sufficient examination was performed, the tumor was difficult to diagnose as being a metastatic tumor or a choroid plexus carcinoma. Because of this, we performed endoscopic biopsy of the intraventricular tumor. However intraoperative findings were not helpful in distinguishing metastatic tumor and choroid plexus carcinoma. Postoperatively, histological examination was performed. However it was still difficult to differentiate this rare tumor from choroid plexus carcinoma by only hematoxylin and eosin stain. For further examination, Ber EP-4 stain was performed. Ber EP-4 showed strongly positive which indicates metastatic tumor. This method led us to make an appropriate diagnosis of this extremely rare tumor.

We considered that in order to diagnose this rare tumor, appropriate histopathological examination, including immunohistopathological examination should be performed.

(Received : March 10, 2011, Accepted : April 25, 2011)

No Shinkei Geka 39(10): 991 - 997, 2011

I. はじめに

脈絡叢乳頭腫や脈絡叢乳頭癌は比較的稀な脳腫瘍である。その発生頻度は人口10万人当たり0.3人に発生するといわれ^{9,10)}, 全脳腫瘍のうち0.4~0.8%³⁰⁾を占めるに過ぎない。一方で、頭蓋外原発の悪性腫瘍の脈絡叢転移も極めて稀である。

われわれが渉猟し得た限りでは、過去に35例の報告^{3,7,13,20,23-26,28,29)}しかない。この35例のうち、原発巣としては腎癌の報告²³⁻²⁶⁾が最も多く、次いで肺・大腸^{7,24)}と続いている。しかし、胆管細胞癌からの転移は過去に報告例はない。両者の鑑別はその稀少性ゆえに時として臨床所見(画像所見)、病理所見において困難を伴う。

*(2011. 3. 10 受稿, 2011. 4. 25 受理)

1) 北海道大学病院脳神経外科, Department of Neurosurgery, Hokkaido University Hospital

2) 同 病理部, Department of Pathology, Hokkaido University Hospital

[連絡先] 栗栖宏多=北海道大学病院脳神経外科 (☎060-8648 札幌市北区北14条西5丁目)

Corresponding author : Kota KURISU, M.D., Department Neurosurgery, Hokkaido University Hospital, North-14 West-5, Kitaku, Sapporo-city, Hokkaido 060-8648, JAPAN

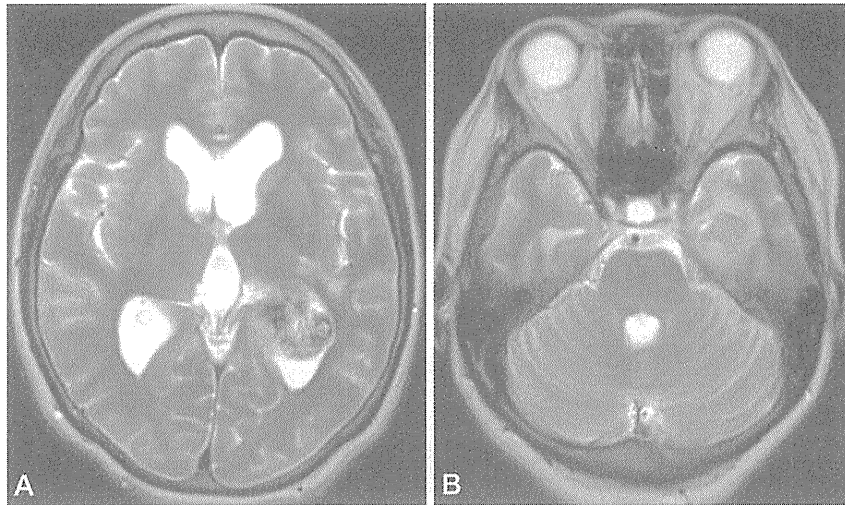


Fig. 1 T2 weighted imaging on admission. A: Intraventricular tumor in the left trigone demonstrated mixed intensity. And the tumor was accompanied with peritumoral edema. B: The tumor located in the left inferior horn was observed.

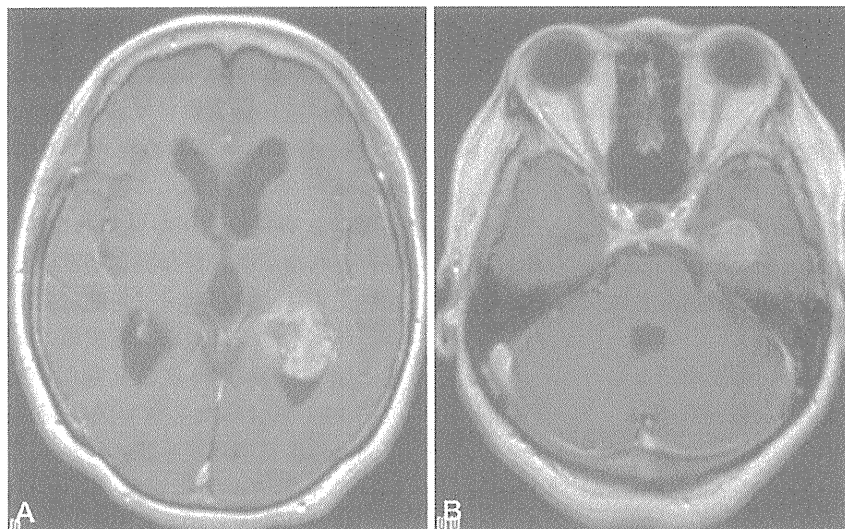


Fig. 2 T1 weighted image after administration of gadolinium. A: The tumor was strongly enhanced. B: The tumor located in the left inferior horn was also strongly enhanced.

今回、われわれは成人担癌患者（胆管細胞癌）に側脳室内脈絡叢部に腫瘍が認められた症例を経験した。画像所見、病理所見を含め原発性腫瘍、転移性腫瘍の鑑別が問題となったが、病理組織診断を用いて最終診断として転移性腫瘍との診断に至った。この非常に稀であり、診断に難渋した症例をその診断過程も含めて若干の文献的考察を加

えて報告する。

II. 症 例

〈患者〉 57歳 女性

現病歴 2010年6月に前医外科にて肝内胆管細胞癌に対する根治術を施行された。前医での病

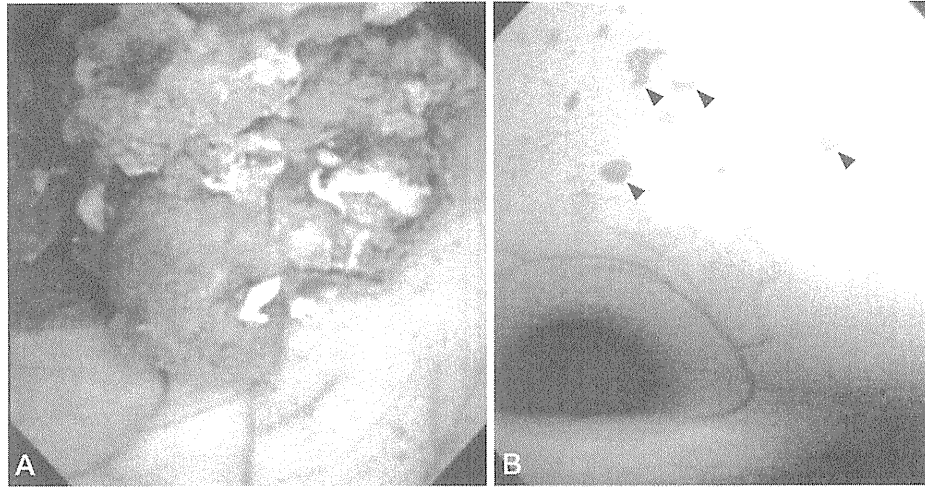


Fig. 3 Intraoperative photographs. A: The intraventricular tumor was reddish and soft, partly calcified and highly vascular and originated from the choroid plexus. B: In the 3rd ventricle, disseminated lesions (arrow heads) were observed.

理組織診断にて胆管細胞癌 (tubular adenocarcinoma) で脈管侵襲はなく、断端陰性と診断された。術後明らかな再発や転移は指摘されず、外来経過観察中であった。

2010年9月、偶発的に前医脳神経外科で施行された頭部 magnetic resonance imaging (MRI) にて、側脳室内腫瘍性病変が指摘され、当科に紹介となった。

神経学的陽性所見 特記事項なし

血液生化学的評価 各種腫瘍マーカーは alpha fetoprotein (AFP) : 3.1 ng/mL (基準値 1.0 ~ 10.0 ng/mL), carcinoembryonic antigen (CEA) : 3.1 ng/mL (基準値 1.0 ~ 6.5 ng/mL), carbohydrate antigen 19-9 (CA19-9) : 63.0 U/mL (基準値 0 ~ 37 U/mL), squamous cell carcinoma (SCC) 抗原 : 0.7 ng/mL (基準値 0 ~ 1.5 ng/mL) と CA 19-9 の高値を認めた。また髄液細胞診断からは異常形態を示す細胞は検出されなかった。

画像評価 当院にて撮像を行った頭部 computed tomography (CT) では、左側脳室内三角部に石灰化を伴った腫瘍性病変を認め、同様に同側下角先端部にも石灰化を伴った腫瘍性病変が認められた。MRI ではこれらの腫瘍性病変は不整形で脳実質とはほぼ等信号を示し、腫瘍内部には T2 強

調画像 (Fig. 1) で低信号領域が散在していた。同腫瘍は隣接脳実質に浸潤傾向を示し、gadolinium 造影像では腫瘍は不均一で著明な増強効果を伴っていた (Fig. 2)。このほか第四脳室 Luschka 孔部にも病変の存在が疑われた。全脊髄 MRI も施行されたが明らかな腫瘍病変は認めなかった。

以上より、左側脳室三角部に発生した転移性脈絡叢腫瘍もしくは脈絡叢乳頭癌の頭蓋内播種性病変と考え、腫瘍病変の全身検索を目的として FDG-PET を含めた各種画像評価を行ったが、頭蓋内以外に腫瘍病変を認めなかった。頭蓋内腫瘍病変は全摘出が困難であることから、原発性病変、転移性病変の両者を考慮した、全脳全脊髄照射を本段階で行うことも検討したが、患者側からの病理組織診断への強い希望もあり、2010年10月、内視鏡下脳室内腫瘍生検術を実施した。術中所見では易出血性、脆弱な腫瘍性病変を脳室三角部脈絡叢に認め、同時に側脳室、第三脳室内に播種性病変を認めた (Fig. 3)。同脈絡叢部の腫瘍の病理組織診断を行った。

病理組織所見 病理学的には腫瘍は hematoxylin-eosin (H.E.) 染色で異型の強い核を有する細胞が乳頭状増生を示し、脈絡叢乳頭癌として矛盾しない所見であったが (Fig. 4)、後日追加で行っ

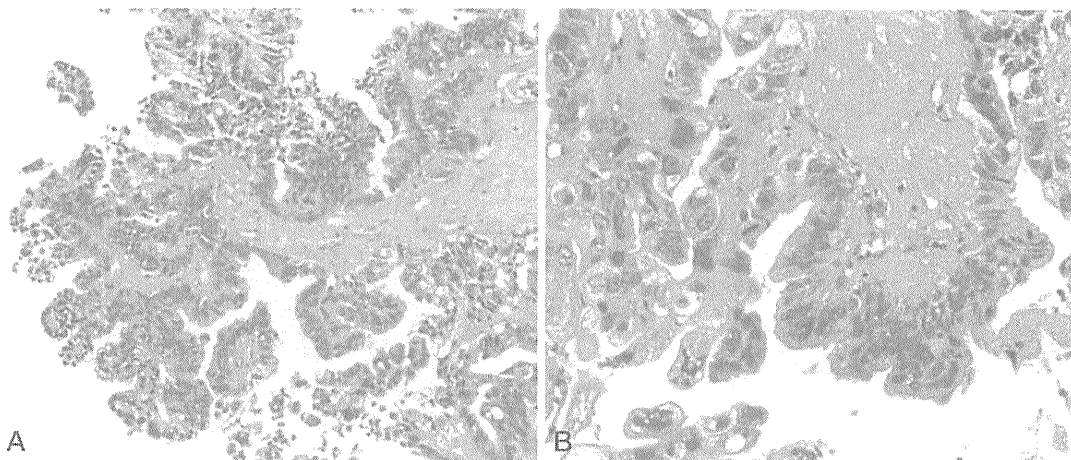


Fig. 4 Histopathological photographs (hematoxylin and eosin stain). A: low magnification, B: high magnification. Tumor with a papillary configuration was observed, and a pleomorphic nucleus was also observed.

た免疫染色にて glial fibrillary acidic protein (GFAP) 陰性, transthyretin 陰性, S100 protein 陰性であり, 脈絡叢乳頭癌としては非典型的であり, Ber-EP4 の免疫染色を追加したところ正常脈絡叢との境界が明瞭な陽性を示し, 最終的に胆管細胞癌の脈絡叢転移と診断した (Fig. 5). 患者は確定診断後, 放射線治療により全脳全脊髄照射 (30.6 Gy+boost 14.4 Gy) を行い, 現在は経過観察中である.

III. 考 察

脳室内腫瘍の発生頻度は比較的稀であり, その診断には難渋することが多い. 今回, われわれは術前には確定診断に至らず, 生検術を行い, 過去に報告例のない胆管細胞癌の脈絡叢転移と診断できた1例を経験した.

胆管細胞癌は比較的稀な消化器悪性腫瘍であり^{12,16)}, その発生頻度は10万人当たり1~2人に発症する²²⁾といわれ, 胃腸器系に発生する癌の3%²⁷⁾を占める. 一般に転移性脳腫瘍は癌治療の進歩, 癌年齢人口の増加に伴いその頻度が増加しており, Kaalら¹¹⁾は担癌患者の25%に認めると報告している. しかし脈絡叢転移は比較的稀であり, その頻度は, 頭蓋外悪性腫瘍にて死亡した737例の剖検例の検討によっても2.6%にしか認められないという報告²¹⁾がある. さらにAl-Anaziら¹⁾

とKohnoら¹⁵⁾によると, 脳室内腫瘍そのものの頻度が低い中で転移性腫瘍は6%に過ぎず, また頭蓋内転移性腫瘍のうち脈絡叢転移は0.14%と極めて稀である. 脈絡叢の転移性腫瘍の報告は渉猟し得るもので過去35例^{3,7,13,20,23-26,28,29)}を認めるのみであり, 自験例を加えても36例に過ぎない. この中で, 臓器別の腫瘍原発巣は, 多い順より腎臓16例 (44.4%)²³⁻²⁶⁾, 肺4例 (11.1%)^{7,24)}, 大腸4例 (11.1%)²⁴⁾, 甲状腺3例 (8.3%)^{3,28,29)}の報告を認めた. しかしながら本症例のように胆管細胞癌の脳室内, 脈絡叢転移の報告は認めず, 本報告が初めてのものとなる. この稀少性から, 本症例では術前の臨床所見や画像所見から診断に至らず, 病理組織診断においても確定診断に難渋した.

一般に側脳室内腫瘍を認めた場合, 髄膜腫や上衣腫, 悪性リンパ腫などさまざまな原発性腫瘍性病変が鑑別疾患として挙げられるが, 本症例においては転移性脈絡叢腫瘍と脈絡叢乳頭癌の鑑別が問題となった. 本症例で患者は, 受診時に胆管細胞癌の既往は既知の情報であったが, FDG-PETを含めた各種全身検索では脳室内腫瘍以外に明らかな腫瘍性病変は認めなかった. 一方, 胆管細胞癌の腫瘍マーカーとして汎用されている血清CA19-9は異常高値を示しており, 胆管細胞癌の再発もしくは転移性腫瘍の存在を示唆する所見であった^{12,16)}が, 胆管細胞癌の術後であること, ま

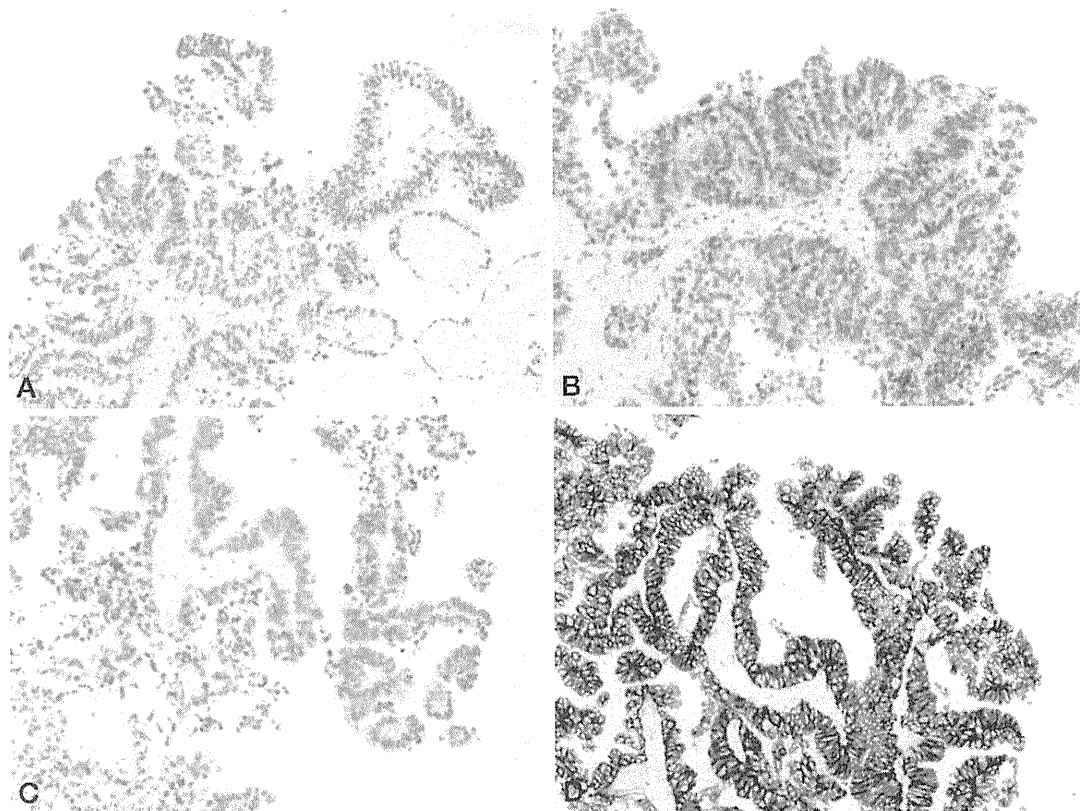


Fig. 5 Immunohistochemical examination. A: GFAP, B: S100 protein, C: transthyretine, D: Ber EP-4

た脈絡叢乳頭癌でも高値を示すとする報告^{8,17)}もあり、両者の鑑別における決定的な所見とはいえなかった。画像所見上も左側脳室内後角に分葉状の強い増強効果を示す病変があり、さらに下角先端部や第四脳室左側 Luschka 孔に沿った多発性の病変を認め、隣接脳実質への浸潤性の変化も認めており、脈絡叢の転移性腫瘍、もしくは脈絡叢乳頭癌どちらにおいても矛盾しない所見であった。このため両者を病理組織診断なしに鑑別することは困難であった。

さらに本症例の病理組織診断では、H.E. 染色標本上も組織像として脈絡叢乳頭癌としても矛盾しない所見が得られており、病理医においても転移性腫瘍と脈絡叢乳頭癌の鑑別に時間を要した。診断に際して脈絡叢乳頭癌の免疫染色法には多数の報告があるが、感度・特異度の高いものに関してはまだ議論の余地がある^{2,4,18,19)}。その一方で脈

絡叢原発性腫瘍と転移性腫瘍との病理学的な鑑別に関しては、いくつかの免疫染色法の報告があり^{5,6,14)}、Kepes ら¹⁴⁾は synaptophysin による免疫染色がこの鑑別に有効とも報告しているが、本症例では行わなかった。また、Gyure ら⁶⁾は cytokeratin (CK) 7 と CK20 を用いた脈絡叢原発性腫瘍と転移性脈絡叢腫瘍の鑑別について報告している。しかし本症例では、既往としてあった胆管細胞癌の CK7/CK20 のフェノタイプは、脈絡叢原発性腫瘍の大半 (74%) を示す CK7 positive/CK20 negative と一致しており、鑑別に有用でなかった。このほかにも腫瘍マーカーである CEA¹⁸⁾ や CA19-9¹⁷⁾ の免疫染色が鑑別に有用であるという報告があるが、これは脈絡叢原発性腫瘍の診断に CEA や CA19-9 の免疫染色が有用であったという報告であり、胆管細胞癌の既往がある本症例では有効ではなかった。Gottschalk ら⁵⁾は上皮性抗原である

HEA125 と Ber EP-4 は、非常に高い感度で脈絡叢原発性腫瘍（脈絡叢乳頭腫，脈絡叢乳頭癌）と脈絡叢の転移性腫瘍を鑑別できると報告している。本症例では、各種免疫染色にて GFAP 陰性，transferrin 陰性，S100 protein 陰性であり，Ber-EP4 の免疫染色を追加したところ正常脈絡叢と境界明瞭に陽性を示し，胆管細胞癌の脈絡叢転移との診断に至っており，同免疫染色法の高い有用性が認められた。今後，自験例のようなケースにおいて考慮すべき染色法である。

IV. 結 語

今回われわれは，側脳室内脈絡叢に認められた稀な胆管細胞癌転移性腫瘍を経験した。画像所見，病理所見上の診断は困難であったが，Ber-EP4 免疫染色を追加することによって，最終診断が可能であった。

文 献

- 1) Al-Anazi A, Shannon P, Guha A : Solitary metastasis to the choroid plexus. Case illustration. *J Neurosurg* **92** : 506, 2000
- 2) Coffin CM, Wick MR, Braun JT, Dehner LP : Choroid plexus neoplasms. Clinicopathologic and immunohistochemical studies. *Am J Surg Pathol* **10** : 394-404, 1986
- 3) Ferrer Garcia JC, Merino Torres JF, Ponce Marco JL, Pinon Selles F : Unusual metastasis of differentiated thyroid carcinoma [In Spanish]. *An Med Interna* **19** : 579-582, 2002
- 4) Gopal P, Parker JR, Debski R, Parker JC : Choroid plexus carcinoma. *Arch Pathol Lab Med* **132** : 1350-1354, 2008
- 5) Gottschalk J, Jautzke G, Paulus W, Goebel S, Cervos-Navarro J : The use of immunomorphology to differentiate choroid plexus tumors from metastatic carcinomas. *Cancer* **72** : 1343-1349, 1993
- 6) Gyure KA, Morrison A : Cytokeratin 7 and 20 expression in choroid plexus tumors : Utility in differentiating these neoplasms from metastatic carcinoma. *Mod Pathol* **13** : 638-643, 2000
- 7) Healy JF, Rosenkrantz H : Intraventricular metastasis demonstrated by cranial computed tomography. *Radiology* **136** : 124, 1980
- 8) Inamura T, Nishio S, Miyagi Y, Kamikaseda K, Ueda K, Fukui M, Yoshimoto K : Primary choroid plexus carcinoma producing carbohydrate antigen 19-9. *Clin Neuropathol* **19** : 268-272, 2000
- 9) Janisch W, Staneczek W : Epidemiology of tumors of the central nervous system – influence of the autopsy rate on the incidence rate. *Arch Geschwulstforsch* **58** : 51-55, 1988
- 10) Janisch W, Staneczek W : Primary tumors of the choroid plexus : Frequency, localization and age. *Zentralbl Allg Pathol* **135** : 235-240, 1989
- 11) Kaal EC, Niel CGJH, Vecht CJ : Therapeutic management of brain metastasis. *Lancet Neurol* **4** : 289-298, 2005
- 12) Kahn SA, Thomas HC, Davidson BR, Taylor-Robinson SD : Cholangiocarcinoma. *Lancet* **366** : 1303-1314, 2005
- 13) Kendall B, Reider-Grosswasser I, Valentine A : Diagnosis of masses presenting within the ventricles on computed tomography. *Neuroradiology* **25** : 11-22, 1983
- 14) Kepes JJ, Collins J : Choroid plexus epithelium (normal and neoplastic) expresses synaptophysin. A potentially useful aid in differentiating carcinoma of the choroid plexus from metastatic papillary carcinomas. *J Neuropathol Exp Neurol* **58** : 398-401, 1999
- 15) Kohno M, Matsutani M, Sasaki T, Takakura K : Solitary metastasis to the choroid plexus of the lateral ventricle : report of three cases and a review of the literature. *J Neurooncol* **27** : 47-52, 1996
- 16) Mosconi S, Bretta GD, Labianca R, Zampino MG, Gatta G, Heinemann V : Cholangiocarcinoma. *Hematology* **69** : 259-270, 2009
- 17) Osada H, Mori K, Yamamoto T, Nakao Y, Wada R, Maeda M : Choroid plexus carcinoma secreting carbohydrate antigen 19-9 in an adult. *Neurol Med Chir (Tokyo)* **46** : 251-253, 2006
- 18) Paulus W, Janisch W : Clinicopathologic correlations in epithelial choroid plexus neoplasms : a study of 52 cases. *Acta Neuropathol* **80** : 635-641, 1990
- 19) Paulus W, Brandner S : Synaptophysin in choroid plexus epithelial cells : no useful aid in differential diagnosis. *J Neuropathol Exp Neurol* **58** : 1111-1112, 1999
- 20) Puppa AD, Pos SD, Zovato S, Orvieto E, Ciccarino P, Manara R, Zustovich F, Berti F, Gardiman MP, Scienza R : Solitary intra-ventricular brain metastasis from a breast carcinoma. *J Neurooncol* **97** : 123-126, 2010
- 21) Schreiber D, Bernstein K, Schneider J : Metastases of the central nervous system. A third communication. Metastases in the pituitary gland, pineal gland, and choroid plexus. *Zentralbl Allg pathol* **126** : 64-73, 1982
- 22) Shaib YH, El-Serag HB, Davila JA, Morgan R, McGlynn KA : Risk factors of intrahepatic cholangiocarcinoma in the United States : a case-control study. *Gastroenterology* **128** : 620-626, 2005
- 23) Spetzger U, Mull M, Sure U, Gilsbach J : Subarachnoid and intraventricular hemorrhage caused by hypernephroma metastasis, accompanied by innocent bilateral posterior communicating artery aneurysms. *Surg Neurol* **44** : 275-278, 1995
- 24) Sung WS, Dubey A, Erasmus A, Hunn A : Solitary choroid plexus metastasis from carcinoma of the oesophagus. *J Clin Neurosci* **15** : 594-597, 2008
- 25) Tomiyama A, Nakayama H, Aoki K, Ueda M : Solitary metastasis of renal cell carcinoma to the third ventricular choroid

- plexus with rapid clinical manifestation by intratumoral hemorrhage. *Neurol India* 56 : 179-181, 2008
- 26) Toms SA, Suh JH, Weil RJ. Choroid plexus metastasis : *Urology* 70 : 370-371, 2007
- 27) Vauthey JN, Blumgart LH : Recent advances in the management of cholangiocarcinomas. *Semin Liver Dis* 14 : 109-114, 1994
- 28) Wasita B, Sakamoto M, Mizushima M, Kurosaki M, Watanabe T : Choroid plexus metastasis from papillary thyroid carcinoma presenting with intraventricular hemorrhage : case report. *Neurosurgery* 66 : E1213-E1214, 2010
- 29) Zhang YA, Kavar B, Drummond KJ : Thyroid carcinoma metastasis to the choroid plexus of the lateral ventricle. *J Clin Neurosci* 16 : 118-121, 2009
- 30) Zulch KJ : *Brain tumors, their biology and pathology* 1st edition. Springer-Verlag, New York, 1957

Neurohypophyseal germinoma with abundant fibrous tissue

Shunsuke Terasaka · Masahito Kawabori ·
Hiroyuki Kobayashi · Junichi Murata ·
Hiromi Kanno · Shinya Tanaka · Kiyohiro Houkin

Received: 23 May 2011 / Accepted: 13 August 2011
© The Japan Society of Brain Tumor Pathology 2011

Abstract We report an unusual case of neurohypophyseal germinoma with abundant fibrous tissue and clival invasion that was initially misdiagnosed as lymphocytic hypophysitis. A 40-year-old woman presented with diabetes insipidus and panhypopituitarism after delivering her second son and which lasted for 4 years. Magnetic resonance imaging showed the intrasellar mass extending to the suprasellar region with enlarged pituitary stalk. The mass was heterogeneously enhanced and invaded the clivus. Biopsy of the intrasellar mass was performed via the trans-sphenoidal route, and histological examination revealed marked fibrous tissue and infiltration of lymphocytes, with no evidence of tumor cells. Lymphocytic hypophysitis was the initial diagnosis, and corticosteroid therapy was begun. Despite intensive treatment, the lesion enlarged and clinical symptoms worsened 2 weeks after surgery. Subtotal removal of the mass was performed, and a second histological examination revealed typical findings of the germinoma. Subsequently, the patient underwent chemoradiotherapy, and complete remission was achieved. Histological diagnosis is sometimes incorrect in fibrous tumors at the sellar region, and biopsy from several points is strongly recommended for this entity.

Keywords Clival invasion · Fibrous tissue · Germinoma · Hypophysitis · Neurohypophyseal germinoma

Introduction

Intracranial germinomas are malignant neoplasms that constitute 2% of primary brain tumors in Japan; approximately 90% of them occur in patients younger than 30 years [1]. Most patients with neurohypophyseal germinomas present typical clinical symptoms, including diabetes insipidus, hypopituitarism, and visual-field defect [2]. Although magnetic resonance imaging (MRI) with modern sequences may contribute to delineating tumor origin and extent, definitive diagnosis can only be achieved by histological findings—the so-called two-cell pattern, consisting of large neoplastic cells and small lymphocytes. We report a case of neurohypophyseal germinoma that required repeat surgery to reach a definitive diagnosis. The patient presented symptoms of polygalactia, and a mass invaded the clivus. Histological findings of the initial surgery showed predominantly chronic inflammation, with abundant fibrous tissue and no evidence of tumor cells.

S. Terasaka · M. Kawabori · H. Kobayashi (✉) · K. Houkin
Department of Neurosurgery, Hokkaido University Graduate
School of Medicine, North 15 West 7, Kita-ku,
Sapporo 060-8638, Japan
e-mail: hiro-ko@med.hokudai.ac.jp

J. Murata
Sapporo Asabu Neurosurgical Hospital, Sapporo, Japan

H. Kanno · S. Tanaka
Laboratory of Cancer Research, Department of Pathology,
Hokkaido University Graduate School of Medicine,
Sapporo, Japan

Case report

A 40-year-old woman presented with severe headache and double vision and was admitted to our hospital. She had a history of polygalactia after delivering her second son when she was 33 years old. Thirst, polyuria, and amenorrhea followed 3 years after onset. At 39 years old, she had loss of appetite and lost 10 kg. Neurological examination revealed right abducens nerve palsy. Laboratory examination revealed normal serum and urinary electrolyte levels.

Twenty-four-hour urine osmotic pressure was 286 mosm/l (normal 300–1,000), suggesting diabetes insipidus. Baseline endocrine assessment showed thyroid-stimulating hormone (TSH) 0.10 μ IU/ml (normal 0.38–3.64), leuteinizing hormone (LH) <0.1 mIU/ml, follicle-stimulating hormone (FSH) 0.3 mIU/ml, growth hormone (GH) 0.66 ng/ml (normal 0.11–3.90 ng/ml), adrenocorticotropic hormone (ACTH) 20 pg/ml (7–56 pg/ml), free thyroxine (FT₄) 0.84 ng/dl (0.95–1.74 ng/dl), and cortisol 1.0 μ g/dl (4.0–23.3), suggesting panhypopituitarism. All serum tumor markers were negative: alpha-fetoprotein (AFP) 3 ng/ml (normal 0–10 ng/ml), carcinoembryonic antigen (CEA) 4.0 ng/ml (normal 0.0–5.0 ng/ml), and beta-human-chorionic gonadotropin (b-HCG) 0.1 ng/ml (normal 0.0–0.1 ng/ml). Several serum autoimmune antibodies were positive: thyroglobulin antibody 20.7 IU/ml (normal 0–13.6 IU/ml), antithyroid peroxidase antibody 65.1 IU/ml (normal 0–3.2), and antinuclear antibody 80-fold (normal 0- to 20-fold). However, antipituitary antibody was negative. Computed tomography (CT) demonstrated an intrasellar mass extending to the suprasellar region and clivus. Most parts of the mass showed slightly higher density than the surrounding brain parenchyma. No calcification was detected in and around the mass (Fig. 1a). Bone-window sagittal CT scan demonstrated erosion of the sellar floor, dorsum sellae, and upper part of the clivus. MRI showed a somewhat symmetrical intrasellar mass with enlarged pituitary stalk and heterogeneous enhancement (Fig. 1b). Invasion of the cavernous sinus was not evident.

A biopsy of the mass was performed via the transsphenoidal route with the endoscope. After removing mucosae of the sphenoid sinus, the eroded clival bone and the grayish fibrous mass were exposed. The mass was cut at midline, and several pieces of the specimen were taken out for histological evaluation. Then the sella floor was opened widely, and the thickened dura mata was incised in cruciform fashion. The hard mass was cut with microscissors, and specimens were also sampled. Histological investigation revealed predominant lymphocyte infiltration, with a background of fibrous tissue, and showed no evidence of tumor cells (Fig. 2a). Some infiltrated lymphocytes showed positive immunoreactivity for CD3, and most scarcely showed positive for CD20 (Fig. 2b, c). There was no typical granulomatous reaction characterized by the presence of multinucleated giant cells. Lymphocytic hypophysitis was the initial diagnosis, and corticosteroid therapy was begun.

Despite steroid pulse therapy (1,000 mg hydrocortisone with gradient decrease), follow-up MRI 2 weeks after surgery showed marked enlargement of the mass, and the clinical symptom had deteriorated (Fig. 3). The patient underwent a second operation to debulk the mass and obtain further surgical specimens for repeat histological evaluation.

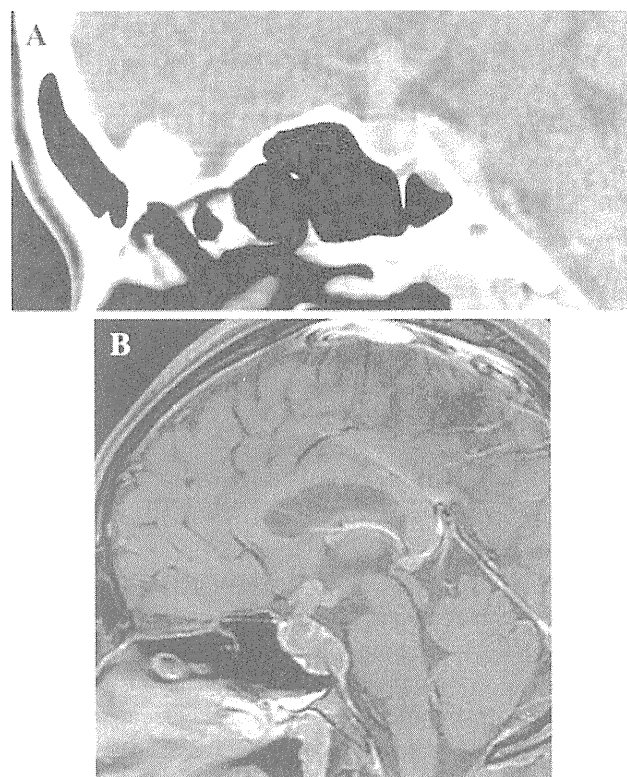


Fig. 1 a A sagittal view of computed tomography (CT) image showing an intrasellar mass extending to the suprasellar and the clivus. The mass shows slightly higher density, and no calcification is detected. b Magnetic resonance imaging with gadolinium diethylenetriamine pentaacetic acid (Gd-DTPA) delineates heterogeneously enhanced intrasellar mass and enlarged pituitary stalk

The second surgery was also performed via the transsphenoidal route. Incision of the mass was made at the midline from the enlarged pituitary stalk to the clivus. Soft tumor tissues appeared inside the mass and were subtotally removed. The operative finding was consistent with that of the germ-cell tumor. Some sections of the second surgery showed typical two-cell patterns, and some showed tumor cells confined within fibrous compartments (Fig. 4a, b). Immunohistochemical staining revealed germ cells positive for placental alkaline phosphatase (PLAP) (Fig. 4c) and c-KIT (CD117). The final pathological diagnosis was pure germinoma.

Subsequently, the patient had combined chemotherapy of iphosphamide (900 mg/m²), cisplatin (20 mg/m²), and etoposide (60 mg/m²) for 5 consecutive days every 4 weeks. After completing four courses of chemotherapy, radiation therapy for whole ventricular systems with total dosage of 25.2 Gy was given in a daily fraction of 1.8 Gy. After chemoradiotherapy, follow-up MRI revealed complete tumor remission. The patient remains well and is on complete hormonal replacement therapy. MRI has shown no tumor recurrence for 3 years.

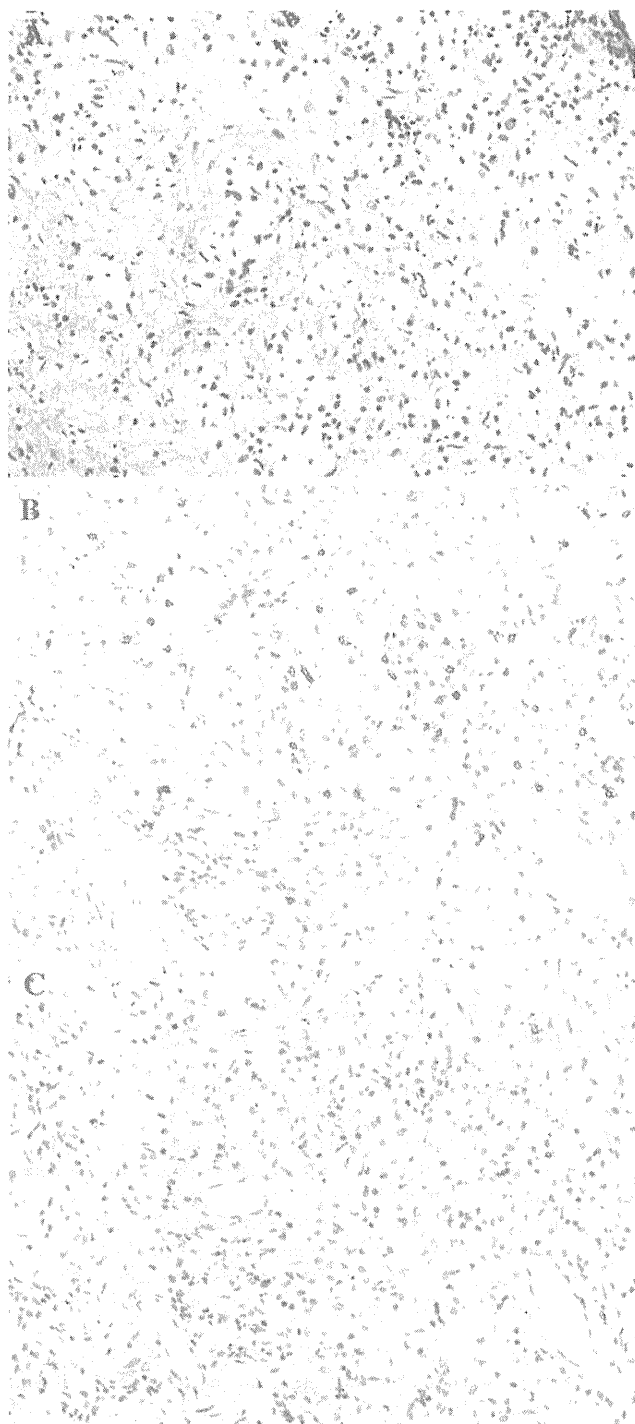


Fig. 2 a Light photomicrograph of the initial specimen showing lymphocytes in abundant fibrous tissue without neoplastic cells. Hematoxylin and eosin (H&E) $\times 400$. b Some lymphocytes showing CD3 immunoreactivity. c Immunostaining for CD20

Discussion

Radiotherapy with/without chemotherapy is now accepted as the gold standard for treating germinoma, and survival at 10 years after diagnosis exceeds 90% [3, 4]. Therefore, the

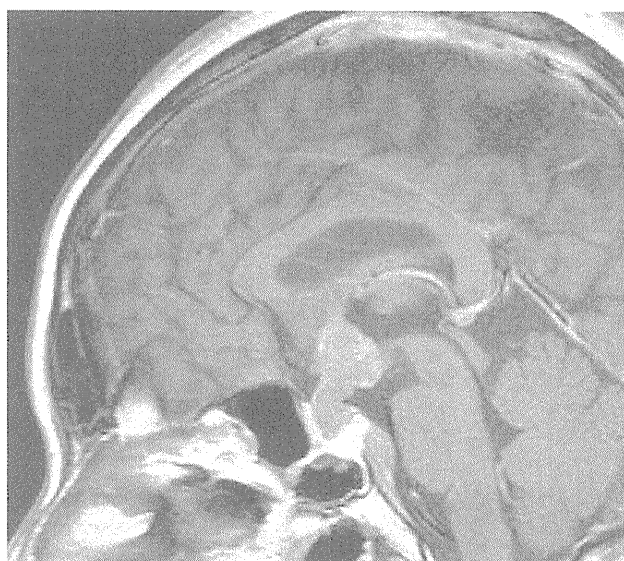


Fig. 3 Sagittal magnetic resonance imaging view with gadolinium diethylenetriamine pentaacetic acid (Gd-DTPA) after the corticosteroid therapy reveal marked enlargement of the mass

primary goal of surgery is to obtain a sufficient volume of tumor tissue for histological examination [5]. In most cases, the diagnosis of germinoma is not difficult because of its typical pathological finding—the so-called two-cell pattern. However, a few cases show unusual pathological findings, with marked fibrous tissue and few or no tumor cells. They are very rarely reported, and authors who do report them emphasize the difficulty in diagnosing this type of germinoma [6–11]. Pathological findings of abundant fibrous tissue and/or granulomatous reaction are not uncommon in seminomas (50–60%) [12] but are observed in only 2.9–4.7% of intracranial germinomas [13–15]. Fibrous tissue in germ-cell tumors is thought to be a reflection of the host immune response to the neoplasm, and the majority of lymphocytes within germinoma tissue are T lymphocytes. Our results of immunohistochemistry using anti-T-cell and anti-B-cell antibodies also indicated infiltrated small-cell T lymphocytes. Controversies remain as to what subsets of T lymphocytes mainly contribute and what factors trigger this phenomenon. Zhao et al. [16] report that tumor-infiltrating lymphocytes in dysgerminoma and seminoma contain high percentage of gamma/delta T cells. Yakirevich et al. [17] report that the presence of increased numbers of activated cytotoxic lymphocytes in testicular seminomas suggests that apoptotic tumor cell death may be triggered by cytotoxic granule effectors. Mueller et al. [18] report an important pathological finding of vital malignant cells gradually replaced transforming to inflammatory granuloma. Chemical mediators, such as tumor necrosis factor-alpha, interferon gamma, and granulocyte-macrophage colony-stimulating factor secreted by

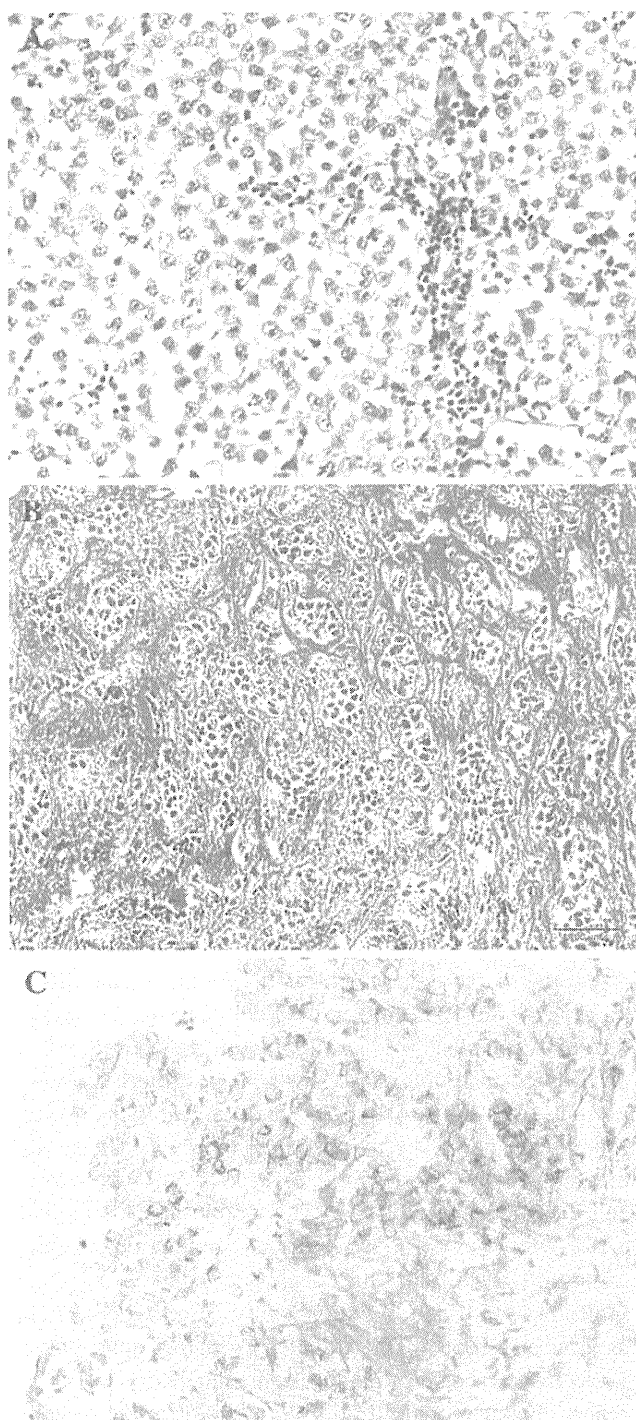


Fig. 4 **a** Photomicrograph of the second surgical specimen shows typical the two-cell pattern. Hematoxylin and eosin (H&E) $\times 400$. **b** Tumor cells are confined within fibrous compartment. Masson Trichrome stain $\times 100$. **c** Tumor cells are positive for immunohistochemical staining with placental alkaline phosphatase (PLAP) $\times 400$

T cells represent a spontaneous cytotoxic capacity against tumor cells and thus may play a role in regulating tumor proliferation and in tumor surveillance [19]. Participation of the transforming growth factor- β and interleukin-13 was

also suggested to develop fibrous tissue and granuloma [20]. The absence of the lymphatic system in the brain might explain why the fibrous tissue and granulomatous reactions are rare in intracranial germinoma.

In our case, several factors led us to the initial misdiagnosis. The patient was relatively old for this type of tumor; only 50 patients out of 1,246 with germinoma registered in Japan between 1984 and 2000 [1] were >40 years (4%). The patient's polygalactia occurred immediately after delivering her second son, and panhypopituitarism and diabetes insipidus followed 3 years after its onset. These clinical symptoms are unusual in germinoma. Positive antinuclear antibody in laboratory examination and predominant lymphocyte infiltration with a background of fibrous tissue in pathological findings also affected our initial diagnosis of the lymphocytic hypophysitis.

Although some papers stress that immunohistochemical staining for c-KIT and PLAP might be useful in granulomatous germinoma diagnosis, [18, 21], we found no cells positive for c-KIT or PLAP in the initial specimen, which was reevaluated after making the final diagnosis. Surgeons should bear in mind that biopsy has a potential risk for misdiagnosis, and several surgical specimens from different points are necessary to reach the correct diagnosis, especially with the hard mass in the suprasellar region.

References

1. The Committee of Brain Tumor Registry of Japan (2009) Report of Brain Tumor Registry of Japan (1984–2000) *Neurol Med Chir* 49(Suppl:i–vii):1–101
2. Horowitz MB, Hall WA (1991) Central nervous system germinomas. A review. *Arch Neurol* 48(6):652–657
3. Ogawa K, Shikama N, Toita T, Nakamura K, Uno T, Onishi H et al (2004) Long-term results of radiotherapy for intracranial germinoma: a multi-institutional retrospective review of 126 patients. *Int J Radiat Oncol Biol Phys* 58(3):705–713
4. Shirato H, Nishio M, Sawamura Y, Myohjin M, Kitahara T, Nishioka T et al (1997) Analysis of long-term treatment of intracranial germinoma. *Int J Radiat Oncol Biol Phys* 37(3):511–515
5. Sawamura Y, Tribolet Nd, Ishii N, Abe H (1997) Management of primary intracranial germinomas: diagnostic surgery or radical resection? *J Neurosurg* 87:262–266
6. Konno S, Oka H, Utsuki S, Kondou K, Tanaka S, Fujii K et al (2002) Germinoma with a granulomatous reaction. Problems of differential diagnosis. *Clin Neuropathol* 21(6):248–251
7. Utsuki S, Oka H, Tanizaki Y, Kondo K, Kawano N, Fujii K (2006) Histological features of intracranial germinomas not disappearing immediately after radiotherapy. *Neurol Med Chir (Tokyo)* 46(9):429–433
8. Fukushima T, Takemura Y, Tsugu H, Iwaasa M, Nabeshima K, Takano K et al (2007) Neurohypophyseal granulomatous germinoma invading the right cavernous sinus: case report and review of the literature. *Pediatr Neurosurg* 43(4):297–302
9. Utsuki S, Oka H, Tanizaki Y, Kondo K, Kawano N, Fujii K (2005) Pathological features of intracranial germinomas with

- reference to fibrous tissue and granulomatous change. *Brain Tumor Pathol* 22(1):9–13
10. Endo T, Kumabe T, Ikeda H, Shirane R, Yoshimoto T (2002) Neurohypophyseal germinoma histologically misidentified as granulomatous hypophysitis. *Acta Neurochir (Wien)* 144(11):1233–1237
 11. Gotoda H, Fujita M, Inoue K, Sawamura Y, Tada M, Abe H et al (1996) Cerebral germinoma with marked granulomatous inflammation: granulomatous germinoma. *Neuropathology* 16:165–171
 12. Sung MT, MacLennan GT, Cheng L (2006) Retroperitoneal seminoma in limited biopsies: morphologic criteria and immunohistochemical findings in 30 cases. *Am J Surg Pathol* 30(6):766–773
 13. Friedman NB (1947) Germinoma of the pineal; its identity with germinoma (seminoma) of the testis. *Cancer Res* 7(6):363–368
 14. Bjornsson J, Scheithauer BW, Okazaki H, Leech RW (1985) Intracranial germ cell tumors: pathobiological and immunohistochemical aspects of 70 cases. *J Neuropathol Exp Neurol* 44(1):32–46
 15. Pickard WR, Clark AH, Abel BJ (1983) Florid granulomatous reaction in a seminoma. *Postgrad Med J* 59:334–335
 16. Zhao X, Wei YQ, Kariya Y, Teshigawara K, Uchida A (1995) Accumulation of gamma/delta T cells in human dysgerminoma and seminoma: roles in autologous tumor killing and granuloma formation. *Immunol Invest* 24(4):607–618
 17. Yakirevich E, Lefel O, Sova Y, Stein A, Cohen O, Izhak OB et al (2002) Activated status of tumour-infiltrating lymphocytes and apoptosis in testicular seminoma. *J Pathol* 196:67–75
 18. Mueller W, Schneider GH, Hoffmann KT, Zschenderlein R, von Deimling A (2007) Granulomatous tissue response in germinoma, a diagnostic pitfall in endoscopic biopsy. *Neuropathology* 27(2):127–132
 19. Vaquero J, Coca S, Magallon R, Ponton P, Martinez R (1990) Immunohistochemical study of natural killer cells of tumor infiltrating lymphocytes of primary intracranial germinoma. *J Neurosurg* 72:619–625
 20. Lee CG, Homer RJ, Zhu Z, Lanone S, Wang X, Koteliansky V et al (2001) Interleukin-13 induces tissue fibrosis by selectively stimulating and activating transforming growth factor beta (1). *J Exp Med* 194:809–821
 21. Mori R, Nakajima M, Sakai H, Fukunaga M, Abe T (2008) Pineal germinoma with a prominent epithelioid cell granuloma component: case report. *Neurol Med Chir (Tokyo)* 48(12):573–575

A possible mechanism of isolated oculomotor nerve palsy by apoplexy of pituitary adenoma without cavernous sinus invasion: a report of two cases

Hiroyuki Kobayashi · Masahito Kawabori ·
Shunsuke Terasaka · Junichi Murata · Kiyohiro Houkin

Received: 4 February 2011 / Accepted: 12 September 2011
© Springer-Verlag 2011

Abstract Isolated oculomotor nerve palsy occasionally occurs in patients with cavernous sinus invasion with or without pituitary apoplexy. We describe two cases of pituitary apoplexy without cavernous sinus invasion presenting with isolated oculomotor palsy. In both cases, computed tomography (CT) showed erosion of the right posterior clinoid process. Magnetic resonance imaging (MRI) depicted pituitary adenoma with apoplexy protruding latero-posteriorly to the right cavernous sinus. The medio-posterior wall of the cavernous sinus was markedly displaced latero-posteriorly by the tumor, and there was no evidence of cavernous sinus invasion. Oculomotor palsy may be caused first by unilateral erosion of the posterior clinoid process, resulting in latero-posterior protrusion of the adenoma. Hemorrhage may result in sudden kinking of the oculomotor nerve at the entrance of the oculomotor trigone.

Introduction

Pituitary adenomas classically present with visual field defects initially, i.e., bitemporal hemianopsia, and cause ophthalmoplegia only late in their clinical course. Isolated

oculomotor nerve palsy is a well-documented symptom of pituitary apoplexy [4]. It is assumed that a sudden increase of pressure in the cavernous sinus caused by apoplexy may compress the oculomotor nerve. In this report, we describe two cases of isolated oculomotor nerve palsy associated with pituitary apoplexy. However, in both cases the tumor did not invade the ipsilateral cavernous sinus. We discuss the probable pathogenesis of isolated oculomotor nerve palsy in this rare condition.

Case reports

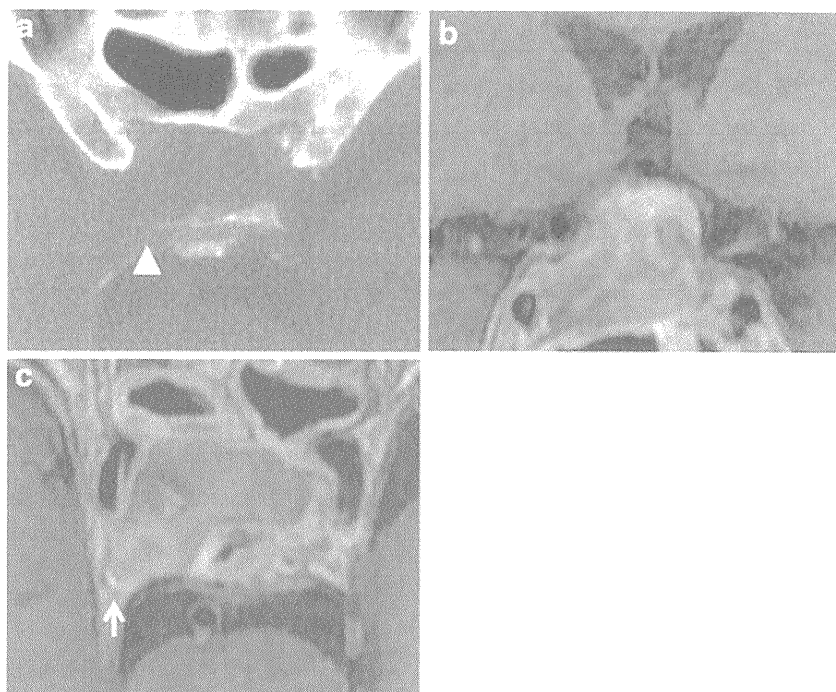
Case 1

An 82-year-old man was admitted to our hospital with complaints of headache, malaise, nausea, and right eye ptosis. He had a complete right oculomotor nerve palsy, with a pupil 8 mm in diameter that was poorly responsive to light. A detailed visual field test was unremarkable. Computed tomography (CT) demonstrated a rounded hetero-dense mass at the pituitary fossa, and bone window CT (Fig. 1a) showed erosion of the right posterior clinoid process. Magnetic resonance imaging (MRI) (Fig. 1b, c) further confirmed the presence of a lobulated pituitary tumor with acute hemorrhage, and the pituitary tumor extended latero-posteriorly to the right cavernous sinus. Magnetic resonance angiography (MRA) excluded an intracranial aneurysm. The patient underwent endoscopic assisted trans-sphenoidal surgery (TSS) 9 days after onset of symptoms. Intraoperatively, the medio-posterior wall of the cavernous sinus was found to be markedly displaced by the tumor; however, there was no evidence of cavernous sinus invasion of the tumor. The tumor was completely resected, and the oculomotor nerve

H. Kobayashi · M. Kawabori · S. Terasaka (✉) · K. Houkin
Department of Neurosurgery,
Hokkaido University Graduate School of Medicine,
North 15 West 7,
Kita-ku, Sapporo 060-8638, Japan
e-mail: terasas@med.hokudai.ac.jp

J. Murata
Sapporo Azabu Neurosurgical Hospital,
Sapporo, Japan

Fig. 1 CT and MRI of patient 1. Bone window CT (**a**) shows erosion of the right posterior clinoid process (*arrowhead*). Gd-enhanced T1-weighted MRI (Gd-T1) (**b** coronal, **c** axial) showing a heterogeneous pituitary mass that represents pituitary apoplexy and protrusion of the tumor latero-posteriorly to the right cavernous sinus (*arrow*)



palsy was fully resolved 3 months after surgery. The pathologic diagnosis was a non-functioning pituitary adenoma.

Case 2

A 52-year-old healthy man presented with sudden headache, nausea, and diplopia. Three days after the onset of symptoms, he was referred to our hospital. On examination, he had an

incomplete right oculomotor nerve palsy, slight blepharoptosis, a 7-mm pupil poorly responsive to light, and moderately impaired adduction of the eye. Fourth and sixth cranial nerve functions were intact and visual fields were full. CT disclosed a hetero-dense pituitary mass, and bone-window CT demonstrated erosion of the right posterior clinoid process (Fig. 2a). MRI identified a hetero-intense pituitary tumor that extended latero-posteriorly to the right cavernous sinus (Fig. 2b, c). He underwent TSS 5 days after onset of symptoms, and the

Fig. 2 CT and MRI of patient 2. Bone-window CT (**a**) demonstrating erosion of the right posterior clinoid process (*arrow*). Gd-T1 MRI (**b** coronal, **c** axial) shows the tumor protruding latero-posteriorly to the right cavernous sinus (*arrowhead*)

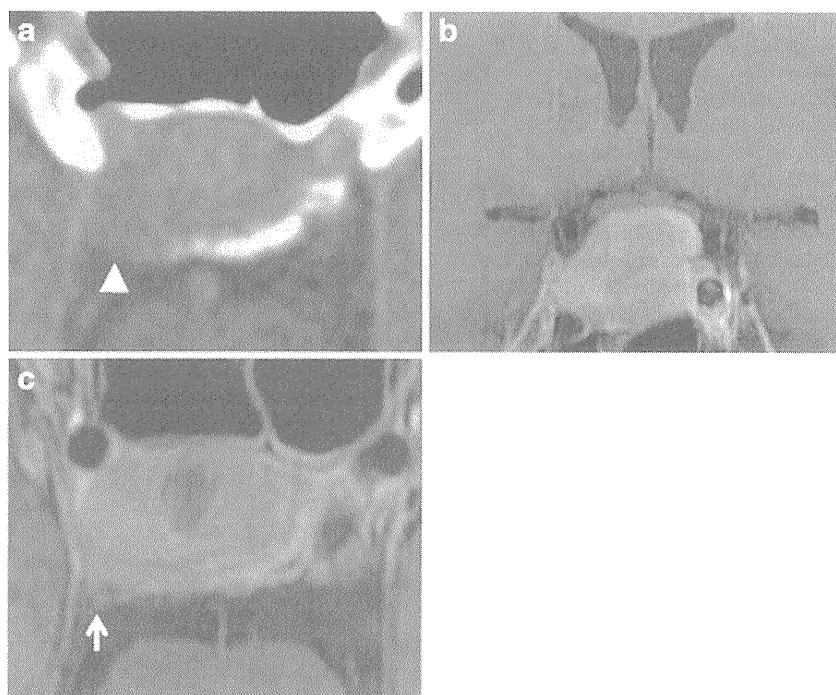


Table 1 Summary of selected studies of pituitary adenoma showing the incidence of isolated oculomotor palsy with apoplexy

Author	Year	Total number of case with pituitary apoplexy	Number of case with isolated third nerve palsy	Reference
Sibal et al.	2004	43	9 (21%)	[5]
Dubuisson et al.	2007	24	12 (50%)	[1]
Kim et al.	2007	12	7 (58%)	[4]
Woo et al.	2010	12	4 (33%)	[7]

pituitary tumor was completely removed. There was no evidence of cavernous sinus invasion of the tumor. Hematoma was detected in the tumor. Immediately after the operation, his right oculomotor nerve function recovered completely. The pathologic diagnosis was a non-functioning pituitary adenoma.

Discussion

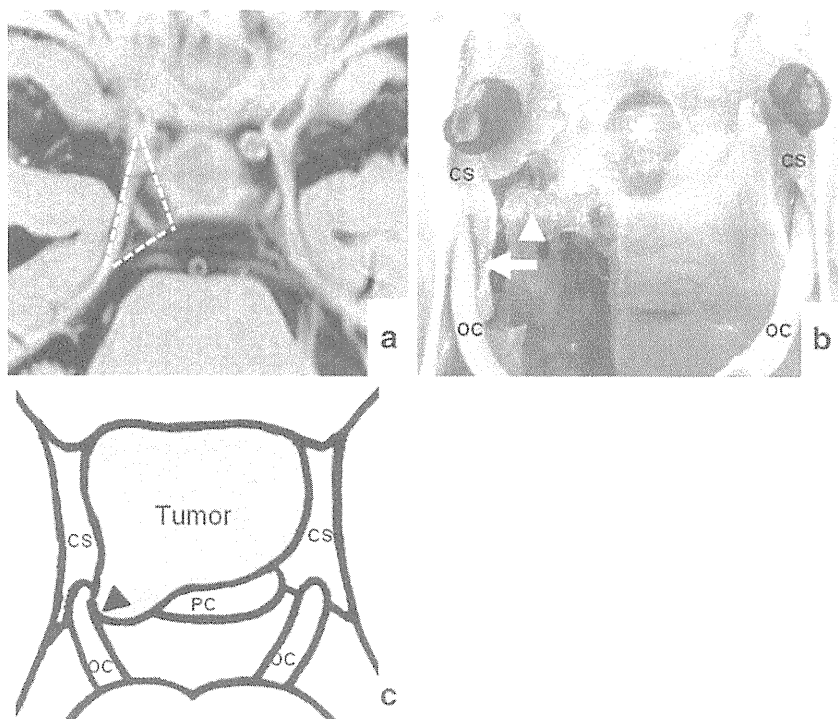
Ocular nerve palsy associated with pituitary tumor has been reported in 2.4-17% of cases. A majority of ocular paresis is due to the third nerve, and the fourth or sixth nerve is rarely affected [4, 7]. Moreover, isolated oculomotor nerve palsy is more frequently observed in pituitary apoplexy (Table 1). Several mechanisms of isolated oculomotor palsy in pituitary adenomas have been proposed. They include direct compression of the nerve by tumor invasion of the cavernous sinus, transmission of pressure on the cavernous sinus wall by tumor expansion, edematous expansion due

to hemorrhage or ischemic infarction of the tumor, direct infiltration of the tumor, and vascular occlusion of the nerve [4]. Each hypothesis is reasonable, especially for cases with cavernous sinus invasion.

In this series, intraoperative endoscopy confirmed that the tumor did not invade the cavernous sinus; instead, it compressed the medio-posterior part of the cavernous sinus and invaginated the cisternal space through the eroded posterior clinoid process, creating a dural pocket. This finding suggested that the third nerve might be compressed proximally where the nerve enters the cavernous sinus from the cistern (Fig. 3b). This anatomical area in the superior wall of the cavernous sinus was defined as the oculomotor trigone, which is limited laterally by the anterior petroclinoid ligament, medially by a line overlying the interclinoid ligament, and posteriorly by the posterior petroclinoid ligament (Fig. 3a) [6]. Dural weakness of the oculomotor trigone has been suggested by Kawase et al. [3]

From an anatomical point of view, compression at this site might be a reasonable cause of isolated oculomotor

Fig. 3 a MRI-CISS (constructive interference in steady-state sequence) depicting the oculomotor trigone (broken line) where the third nerve enters the cavernous sinus from the cistern. b Photographs of the cadaver specimen (left posterior clinoid process without dural coverage) depicting the pituitary gland (asterisk), cavernous sinus (CS), oculomotor nerve (OC) and the posterior clinoid process (white arrowhead). Note that the oculomotor nerve at the oculomotor trigone (arrow) is latero-posterior to the posterior clinoid process. c A scheme of 'hemiation of the adenoma' demonstrates erosion of the posterior clinoid process (PC) by tumor expansion (black arrowhead). Compression of the oculomotor nerve occurs at the oculomotor trigone



nerve palsy. The fourth and sixth nerves must be less affected because the trochlear nerve runs through the tentorial fold [3], and the dural porus in the clivus for the abducens nerve (Dorello's canal) is located approximately 17 mm inferior to the posterior clinoid process [2].

Erosion of the posterior clinoid process with pituitary tumors is not unusual, particularly in macroadenoma. The isolated oculomotor palsy in our cases may result from unilateral erosion of the posterior clinoid process by tumor expansion, which caused latero-posterior protrusion of the adenoma at the fragile dura in the oculomotor trigone (Fig. 3c). Hemorrhage might result in sudden compression or kinking of the oculomotor nerve at the entrance of the oculomotor trigone.

Conclusion

Based on radiological and intraoperative findings, a possible mechanism of isolated oculomotor nerve palsy in pituitary apoplexy in adenomas without cavernous sinus invasion was proposed. Tumor expansion caused unilateral erosion of the posterior clinoid process, resulting in latero-posterior protrusion of the adenoma at the fragile dura in the oculomotor trigone. Then, a sudden increase of intratumoral pressure due to hemorrhage resulted in compression of the oculomotor nerve at the entrance of the oculomotor trigone.

Acknowledgement A photograph of the cadaver specimen (Fig. 3) was kindly provided by the Department of Neurosurgery, Kyorin University.

Conflicts of interest None.

References

1. Dubuisson AS, Beckers A, Stevenaert A (2007) Classical pituitary tumour apoplexy: clinical features, management and outcomes in a series of 24 patients. *Clin Neurol Neurosurg* 109:63–70
2. Iaconetta G, Fusco M, Cavallo LM, Cappabianca P, Samii M, Tschabitscher M (2007) The abducens nerve: microanatomic and endoscopic study. *Neurosurgery* 61:7–14, discussion 14
3. Kawase T, van Loveren H, Keller JT, Tew JM (1996) Meningeal architecture of the cavernous sinus: clinical and surgical implications. *Neurosurgery* 39:527–534, discussion 534–526
4. Kim SH, Lee KC (2007) Cranial nerve palsies accompanying pituitary tumour. *J Clin Neurosci* 14:1158–1162
5. Sibal L, Ball SG, Connolly V, James RA, Kane P, Kelly WF, Kendall-Taylor P, Mathias D, Perros P, Quinton R, Vaidya B (2004) Pituitary apoplexy: a review of clinical presentation, management and outcome in 45 cases. *Pituitary* 7:157–163
6. Umansky F, Valarezo A, Elidan J (1994) The superior wall of the cavernous sinus: a microanatomical study. *J Neurosurg* 81:914–920
7. Woo HJ, Hwang JH, Hwang SK, Park YM (2010) Clinical outcome of cranial neuropathy in patients with pituitary apoplexy. *J Korean Neurosurg Soc* 48:213–218

Comment

Ophthalmoplegias are a slightly more common neurological manifestation of pituitary apoplexy than chiasmal compression symptoms. Not all neurosurgeons are aware of this, and this short report is a reminder. It is important to note that cavernous sinus invasion is not essential to cause these palsies, and the images here illustrate how oculomotor palsies may occur.

Michael Powell
London, UK



Sonodynamic therapy using water-dispersed TiO₂-polyethylene glycol compound on glioma cells: Comparison of cytotoxic mechanism with photodynamic therapy

Shigeru Yamaguchi^a, Hiroyuki Kobayashi^a, Takuhito Narita^a, Koki Kanehira^b, Shuji Sonezaki^b, Nobuki Kudo^c, Yoshinobu Kubota^d, Shunsuke Terasaka^{a,*}, Kiyohiro Houkin^a

^a Department of Neurosurgery, Graduate School of Medicine, Hokkaido University, Sapporo 060-8638, Japan

^b TOTO Ltd. Research Institute, Biotechnology Group, Kita-Kyushu 802-8601, Japan

^c Laboratory of Biological Engineering, Graduate School of Information Science and Technology, Hokkaido University, Sapporo 060-0814, Japan

^d Department of Urology, Graduate School of Medicine, Yokohama-City University, Yokohama 236-0004, Japan

ARTICLE INFO

Article history:

Received 1 June 2010

Received in revised form 26 December 2010

Accepted 27 December 2010

Available online 31 December 2010

Keywords:

Glioma
Fluorescence assay
Photodynamic therapy
Polyethylene glycol
Sonodynamic therapy
Water-dispersed titanium dioxide

ABSTRACT

Sonodynamic therapy is expected to be a novel therapeutic strategy for malignant gliomas. The titanium dioxide (TiO₂) nanoparticle, a photosensitizer, can be activated by ultrasound. In this study, by using water-dispersed TiO₂ nanoparticles, an in vitro comparison was made between the photodynamic and sonodynamic damages on U251 human glioblastoma cell lines. Water-dispersed TiO₂ nanoparticles were constructed by the adsorption of chemically modified polyethylene glycole (PEG) on the TiO₂ surface (TiO₂/PEG). To evaluate cytotoxicity, U251 monolayer cells were incubated in culture medium including 100 µg/ml of TiO₂/PEG for 3 h and subsequently irradiated by ultraviolet light (5.0 mW/cm²) or 1.0 MHz ultrasound (1.0 W/cm²). Cell survival was estimated by MTT assay 24 h after irradiation. In the presence of TiO₂/PEG, the photodynamic cytotoxic effect was not observed after 20 min of an ultraviolet light exposure, while the sonodynamic cytotoxicity effect was almost proportional to the time of sonication. In addition, photodynamic cytotoxicity of TiO₂/PEG was almost completely inhibited by radical scavenger, while suppression of the sonodynamic cytotoxic effect was not significant. Results of various fluorescent stains showed that ultrasound-treated cells lost their viability immediately after irradiation, and cell membranes were especially damaged in comparison with ultraviolet-treated cells. These findings showed a potential application of TiO₂/PEG to sonodynamic therapy as a new treatment of malignant gliomas and suggested that the mechanism of TiO₂/PEG mediated sonodynamic cytotoxicity differs from that of photodynamic cytotoxicity.

© 2011 Elsevier B.V. All rights reserved.

1. Introduction

Sonodynamic therapy (SDT) for cancer is based on the activation of sonosensitizers by ultrasound (US). This is a new approach for cancer therapy derived from photodynamic therapy (PDT). In the treatment of malignant gliomas, there have been several preliminary studies of PDT using 5-aminolevulinic acid (5-ALA), a porphyrin derivative [1–4]. However, the limited tissue penetrability of light has been a crucial problem [5] because the malignant gliomas often develop in deep brain tissue, such as the basal ganglia or the brainstem. In this regard, US can penetrate deeply into tissues and, moreover, can be focused to the tumor site [6–8]. This indicates that SDT with sonosensitizers is expected to become a novel and effective therapeutic arm. Recently, the effects of sonocatalytic

reagents in combination with ultrasound on glioma cells were reported [9,10]. Some photosensitizers such as porphyrin derivatives demonstrate US-induced cytotoxic reactions [11–18].

Titanium dioxide (TiO₂) is also a photosensitizer that has a strong oxidizing activity and produces oxidative radicals under irradiation of ultraviolet (UV) light below 385 nm wavelength [19]. The photocatalytic effect of TiO₂ has been applied to cancer treatment [20–25], and US irradiation is an alternative energy source for TiO₂ [26–28]. Furthermore, toxicological examinations have shown that the TiO₂ nanoparticle is basically nontoxic for experimental cells or animals [29–31]. Therefore, we supposed that sonocatalytic TiO₂ could become a new material in SDT for various cancers involving malignant glioma.

We have developed a novel water-dispersed TiO₂ nanoparticle modified by polyethylene glycole (PEG) and demonstrated its photocatalytic anti-tumor effect on a glioma cell line [32]. These nanoparticle compounds are approximately 50 nm in diameter, and their dispersion and stability in an aqueous medium have been confirmed. These compounds do not cross the blood–brain barrier

* Corresponding author. Address: Department of Neurosurgery, Graduate School of Medicine, Hokkaido University, North 15, West 7, Kita-ku, Sapporo 060-8638, Japan. Tel.: +81 11 706 5987; fax: +81 11 708 7737.

E-mail address: terasas@med.hokudai.ac.jp (S. Terasaka).

(BBB) in normal brain. On the other hand, accumulation of the particles in malignant glioma by transvascular delivery is expected because the normal BBB is disturbed in the tumor site [33,34]. If TiO₂/PEG nanoparticles are activated by US irradiation and lead to damage to the glioma cells, SDT using these nanoparticles might be a novel and safe therapeutic strategy for malignant gliomas.

In the present study, the sonocatalytic cell-killing effect of water-dispersed TiO₂/PEG nanoparticles on the U251 human glioblastoma cell line was evaluated. Then, the role of oxidative radicals generated from excited TiO₂/PEG in tumor cell damage using oxidative radical scavengers was tested, since a previous report speculated that reactive oxidative radicals play a central role in the sonocatalytic process of TiO₂, similar to a photocatalytic effect [26]. Furthermore, the differences between photodynamic and sonodynamic cytotoxicities of this sensitizer were investigated to compare with other reported sensitizers [12,35,36].

2. Materials and methods

2.1. Construction of TiO₂/PEG

The pH of 100 mg/ml comshaped PEG–maleic acid anhydride (PEGMA, AM1510 K; Nihon Yushi Co. Ltd., Tokyo, Japan) dissolved in water was adjusted to 4.0 by 0.1 M NaOH. To activate the carboxyl groups of PEGMA, 0.6 ml of 0.8 mol/l 1-ethyl-3-[3-dimethylaminopropyl] carbodiimide hydrochloride (Pierce, Rockford, IL) was added, and the solution was incubated at room temperature for 5 min. Then, 0.3 ml of 0.2 M 4-amino-salicylic acid (4ASA; Wako Jyunyaku, Osaka, Japan) solution was added, and the mixed solution was incubated at 40 °C for 16 h. Unreacted 4ASA and other small molecules were removed with Amicon Ultra-15 (MWCO = 3000; Millipore, Billerica, MA) by centrifugation five times following the manufacturer's recommendations. Exchange of the solvent of reacted PEGMA–4ASA was carried out after vacuum drying at 25 °C, 20 hPa for 3 min and 5 hPa for 35 min. The concentration of PEGMA–4ASA was adjusted to 50 mg/ml by dimethylformamide (DMF). An acidic TiO₂ sol was prepared by thermal synthesis based on hydrolysis of an organo-titanium compound followed by peptization, as described in detail previously [37]. After hydrolysis of chlorotitanium triisopropoxide (Acros, Morris Plains, NJ), peptization by HNO₃ was carried out at 80 °C. The reactant was adjusted to a solid content of 20% (wt/vol) with 1.5 M HNO₃. After ultrasonication at 200 kHz for 30 min (Midsonic 600; Kaijyo, Tokyo, Japan), particle-size distribution analysis (see "Measurement of particle diameter and zeta-potential" in this section) indicated the presence of approximately 40 nm diameter particles of TiO₂ in the solution. The TiO₂ solution (0.75 ml) was added to 10 ml of DMF, and 5 ml of 50 mg/ml PEGMA–4ASA in DMF was added, followed by stirring. The mixed solution was incubated at 130 °C for 16 h using Chemist Plaza (Shibata Kagaku, Tokyo, Japan). The reaction was carried out under reflux and vigorous stirring at 600 rpm. After the reaction ended, it was cooled to room temperature. Exchange of the solvent of reacted TiO₂/PEG was carried out after vacuum drying at 40 °C, 5 hPa for 10 min. The concentration of TiO₂/PEG was adjusted to 10 mg/ml by water. The TiO₂/PEG aqueous solution was purified with Amicon Ultra-15 (MWCO = 3000; Millipore) by centrifugation five times following the manufacturer's recommendations. Its characteristics were similar to those of the TiO₂/PAA hybrid [38].

2.2. Cell culture

Human glioblastoma cell line U251 was obtained from ATCC® (the American Type Culture Collection, MD, USA). The cells were cultured in vitro in Dulbecco's Modified Eagle Medium (DMEM;

GIBCO™, NY, USA), containing 10% fetal bovine serum (FBS; GIBCO™), 100 U/ml of penicillin and 100 µg/ml of streptomycin (SIGMA®, MO, USA) and MEM non-essential amino acids (GIBCO™), and maintained at 37 °C in a humidified incubator with 5% CO₂ in air.

2.3. UV irradiation

U251 cells (70% confluence) were trypsinized and suspended in DMEM at a concentration of 1×10^5 cells/ml. The cell suspension (100 µl) was plated in each well (1.0×10^4 cells/well) of a 96-well plate (MICROTEST™96, Becton–Dickinson, NJ, USA) and incubated 24 h at 37 °C in humidified air with 5% CO₂. Then, the medium was replaced with 100 µg/ml TiO₂/PEG diluted in fresh DMEM without phenol-red and incubated at 37 °C for 3 h. Phenol red free culture medium was used during UV irradiation to avoid reduction of UV energy as UV penetration is significantly influenced by dyes. After co-incubation, the plates were irradiated with a commercially available UV lamp with a peak wavelength at 360 nm (FL20SS W/18, TOSHIBA, Tokyo, Japan). The light intensity was measured by a coherent power meter (NOVA™, OPHIR, Saitama, Japan). The incident light intensity was 5.0 mW/cm².

2.4. US irradiation

The US apparatus was the commercially available SONIC MASTER ES-2 (OG–Giken, Okayama, Japan). The transducer generates a burst US pulse of 1 MHz center frequency and 100 Hz pulse repetition frequency. The U251 cell suspension (250 µl) was dispensed in a 24-well plate coated with collagen I (BD BioCoat™, BD Bioscience, Bedford, MA, USA), and each well contained approximately 2.5×10^4 cells. Cells were plated, and adjacent wells were not used to avoid the influence of US energy when another well was irradiated. The plates were incubated 24 h at 37 °C in humidified air with 5% CO₂. Then, the medium was replaced by fresh DMEM containing 100 µg/ml of TiO₂/PEG without phenol-red and incubated at 37 °C for 3 h. For the US alone group, the medium was also replaced with fresh DMEM without TiO₂/PEG and phenol red and incubated for the same amount of time. Phenol red free medium was used in the same conditions for UV and US treatment. The plate was placed 20 mm from the surface of the transducer, and 6% acrylamide gel was buffered between the US transducer and the plate to avoid an increase in temperature. The temperature on the plate was checked using TR-K™ (As One, Osaka, Japan), and the temperature was kept less than 37 °C during irradiation. The transducer generated 50% duty-ratio burst US of 0.4–1.2 W/cm² in reading output power. Then the plates were irradiated by US at room temperature separately for each individual well.

According to the measurements by Feril et al. using the same type of US apparatus [40], the peak acoustic pressure and spatial-average-temporal-average intensity (I_{SATA}) of the apparatus were estimated as 0.795 W/cm² and 0.204 MPa, respectively, at reading output intensity of 1 W/cm² with 50% duty ratio. We also confirmed the attenuation of US by 6% acrylamide gel and a base plate of the plastic well inserted between the transducer surface and cells. The measurements were conducted inside a sufficiently large water tank ($0.7 \times 0.5 \times 0.4$ m³) to eliminate the effects of standing wave using a membrane hydrophone (HMB-500, Onda, Sunnyvale, CA, USA). The insertions decreased US pressure and intensity to $86.2 \pm 4.5\%$ and $74.6 \pm 7.8\%$, respectively. In this paper, US intensities are described using values of reading output unless otherwise indicated.

2.5. Cytotoxic assay (MTT assay)

After UV or US irradiation, the treated cells were stored at 37 °C in a humidified incubator with 5% CO₂ in air for 24 h. Cell